LabVIEW Electrocardiogram Event and Beat Detection

MIHAELA LASCU, DAN LASCU
Department of Measurements and Optical Electronics
Faculty of Electronics and Telecommunications
Bd. Vasile Pârvan no.2
ROMANIA
mihaela.lascu@etc.utt.ro, dan.lascu@etc.utt.ro
http://www.etc.upt.ro

Abstract: - QRS and ventricular beat detection is a basic procedure for electrocardiogram (ECG) processing and analysis. Large variety of methods have been proposed and used, featuring high percentages of correct detection. Nevertheless, the problem remains open especially with respect to higher detection accuracy in noisy ECGs. LabVIEW (Laboratory Virtual Instrument Engineering Workbench) is a graphical programming language that uses icons instead of lines of text to create programs. We developed in LabVIEW the filtering for removal of artifacts in biomedical signals and the Pan-Tompkins algorithm. We have investigated problems posed by artifact, noise and interference of various forms in the acquisition and analysis of several biomedical signals. We have also established links between the characteristics of certain epochs in a number of biomedical signals and the corresponding physiological or pathological events in the biomedical systems of concern. Event detection is an important step that is required before we may attempt to analyze the corresponding waves in more detail. A real-time detection method is proposed, based on comparison between absolute values of summed differentiated electrocardiograms of one of more ECG leads and adaptive threshold. Also, a cardiac beat recognition based on continuous wavelet transform is presented.

Key-Words: - biomedical signal, database, electrocardiogram ECG, artifact, noise, graphical programming language LabVIEW, filtering, notch filter, event detection, Pan-Tompkins algorithm, adaptive threshold.

1. Introduction

Biomedical signals are fundamental observations for analyzing the body function and for diagnosing a wide spectrum of diseases.

The problems caused by artifacts in biomedical signals are vast in scope and variety; their potential for degrading the performance of the most sophisticated signal processing algorithms is high.

An ECG signal [1] can be disturbed by a high-frequency noise. The noise could be due to the instrumentation amplifiers, the recording system, and pickup of ambient electromagnetic signals by the cables. The signal illustrated has also been corrupted by power-line interference at 60Hz and its harmonics, which may also be considered as a part of high-frequency noise relative to the low-frequency nature of the ECG signal.

Low-frequency artifacts and base-line drift may be caused in chest-lead ECG signals by coughing or breathing with large movement of the chest. Poor contact and polarization of the electrodes may also cause low-frequency artifacts. Base line drift may sometimes be caused by variations in temperature and bias in the instrumentation and amplifiers as well.

The most commonly encountered periodic artifact in biomedical signals is the power-line interference at 50Hz or 60Hz. If the power-line waveform is not a pure sinusoid due to distortions or clipping, harmonics of the fundamental frequency could also appear. Harmonics will also appear if the interference is a periodic waveform that is not a sinusoid. Power-line interference may be difficult to detect visually in signals being non-specific waveforms; however, the interference is easily visible if present on well-defined signal waveforms such as the ECG or carotid pulse signals. In either case, the power spectrum of the signal should provide a clear indication of the presence of power-line interference as an impulse or spike at 50Hz or 60 Hz; harmonics will appear as additional spikes at integral multiples of the fundamental frequency.

If we have an ECG signal recorded from the abdomen of a pregnant woman and simultaneously a recorded ECG from the woman's chest; and we compare these, we see that the abdominal ECG demonstrates multiple peaks corresponding to the maternal ECG as well as several others at weaker levels and higher repetition rate [1].

The non-maternal QRS complexes represent the ECG of the fetus. Observe that the QRS complex

shapes of the maternal ECG from the chest and abdominal leads have different shapes due to the projection of the cardiac electrical vector onto different axes.

The QRS complexes and ventricular beats in an electrocardiogram represent the depolarization phenomenon of the ventricles and yield useful information about their behavior. Beat detection is a procedure preceding any kind of ECG processing and analysis. For morphological analysis this is the reference for detection of other ECG waves and parameter measurements. Rhythm analysis requires classification of QRS and other ventricular beat complexes as normal and abnormal. Real-time ventricular beat detection is essential for monitoring of patients in critical heart condition [1], [3].

2. Filtering for Removal of Artifacts

Information provided by bioelectric signals is generally time-varying, nonstationary, sometimes transient, and usually corrupted by noise. Fourier transform has been the unique tool to face such situations, even if the discrepancy between theoretical considerations and signal properties has been emphasized for a long time. These issues can be now nicely addressed by time-scale and time-frequency analysis [3].

One of the major areas where new insights can be expected is the cardiovascular domain. For diagnosis purpose, the noninvasive electrocardiogram ECG is of great value in clinical practice. The ECG is composed of a set of waveforms resulting from atrial and ventricular depolarization and repolarization. The first step towards ECG analysis is the inspection of P, QRS and T waves Fig.1; each one of these elementary components is a series of onset, offset, peak, valley and inflection points. Ideally, the waves exhibit local symmetry properties with respect to a particular point, peak and inflection points locations of the considered wave. Based on these properties, one can extract significant points to study the wave shapes and heart rate variability.

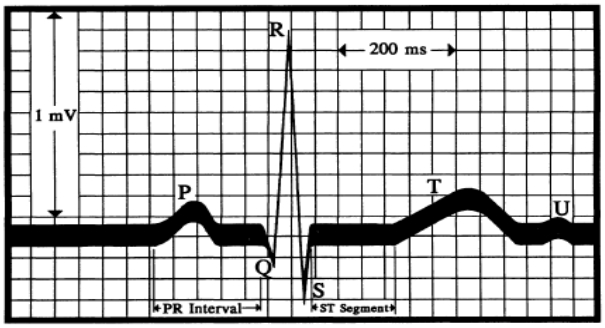

Fig.1. Example of a normal ECG beat.

In our paper we have gained an understanding of a few sources of artifacts in biomedical signals and their nature and we are prepared to look at specific problems and develop effective filtering techniques to solve them. The proposed solution provides the details of an appropriate filtering technique. Certain types of noise may be filtered directly in the time domain using signal processing techniques or digital filters. An advantage of time-domain filtering is that spectral characterization of the signal and noise may not be required. Linear filters fail to perform when the signal and noise spectra overlap. Synchronized signal averaging can separate a repetitive signal from noise without distorting the signal [1]. A synchronized averaging is a type of ensemble averaging. An algorithmic description of synchronized averaging is as follows: a) obtain a number of realizations of the signal or event of interest; b) determine a reference point for each realization of the signal; c) extract parts of the signal corresponding to the events and add them to the buffer, it is possible that the different parts are of different durations; d) divide the result in the buffer by the number of events added.

Let $y_k(n)$ represent one realization of a signal, with $k = 1, 2,\ldots, L$ representing the ensemble index, and $n = 1, 2,\ldots, N$ representing the time-sample index. The observed signal is

$$y_k(n)=x_k(n)+\eta_k(n), \qquad (1)$$

where $x_k(n)$ represents the original uncorrupted signal and $\eta_k(n)$ represents the noise in the k^{ith} copy of the observed signal. If for each instant of time n we add L copies of the signal, we get

$$\sum_{k=1}^{L} y_k(n) = \sum_{k=1}^{L} x_k(n) + \sum_{k=1}^{L} \eta_k(n); \quad n=1,2,\ldots,N. \qquad (2)$$

If the repetitions of the signal are identical and aligned, $\sum_{k=1}^{L} x_k(n) = Lx(n)$. If the noise is random and has zero mean and variance σ_η^2, $\sum_{k=1}^{L} \eta_k(n)$ will tend to zero as L increases, with a variance of $M\sigma_\eta^2$. The RMS value of the noise in the averaged signal is $\sqrt{M}\,\sigma_\eta$. Thus the SNR of the signal will increase by a factor of $\frac{L}{\sqrt{L}}$ or $\sqrt{L}$. The larger the number of epochs or realizations that are averaged, the better will be the SNR of the result.

Fig.2 illustrates two ECG cycles extracted using the trigger points obtained by thresholding the cross-

correlation function [1], as well as the result of averaging the first 11 cycles in the signal.

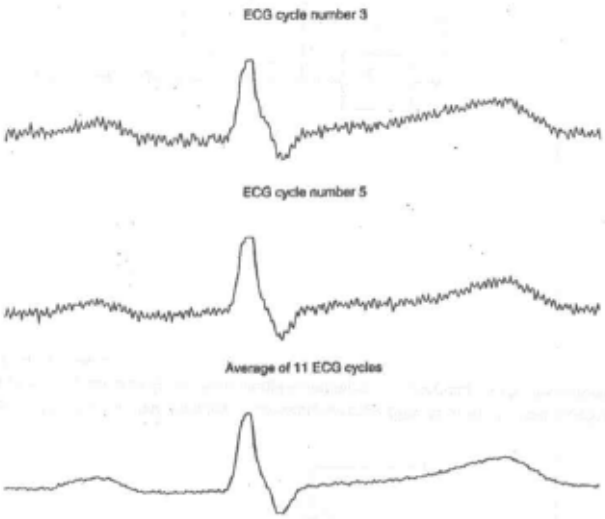

Fig.2. The upper two traces - two cycles of the ECG extracted from an ECG signal with noise. The bottom trace – the result of synchronized averaging of 11 cycles from the same ECG signal.

Structured noise such as power-line interference may be suppressed by synchronized averaging if the phase of the interference in each realization is different.

When an ensemble of several realizations of an event is not available, synchronized averaging will not be possible. In this case we consider temporal averaging for noise removal, with the assumption that the processes involved are ergodic, that is, temporal statistics may be used instead of ensemble statistics.

The biomedical signals, that have been processed, are from Online Biomedical Signals Databases: ftp://ftp.ieee.org/uploads/press/rangayyan, www.ecgdatabase.com, www.ecglibrary.com.

2.1 High frequency noise in the ECG.

The Butterworth filter is perhaps the most commonly used frequency domain filter due to its simplicity and the property of a maximally flat magnitude response in the pass-band [2].

The basic Butterworth lowpass filter function is:

$$\left|H_a(j\Omega)\right|^2 = \frac{1}{1+\left(\frac{j\Omega}{j\Omega_c}\right)^{2N}}\left|H_a\right| \qquad (3)$$

where H_a is the analog filter frequency response, Ω_c is the cutoff frequency in radians/s and N is the order of the filter. As the order N increases, the filter response becomes more flat in the pass-band, and the transition to the stop-band becomes faster or sharper.

Changing to the Laplace variable s, we get:

$$H_a(s) * H_a(-s) = \frac{1}{1+(\frac{s}{j\Omega_c})^{2N}}; \qquad (4)$$

Using the bilinear transformation, that means, by substituting $s = \frac{2}{T}\frac{1-z^{-1}}{1+z^{-1}}$, we obtain the following simplified transfer function:

$$H(z) = \frac{G'\left(1+z^{-1}\right)^N}{\sum_{k=0}^{N} a_k z^{-k}} \qquad (5)$$

where a_k, k=0, 1, 2,…, N, are the filter coefficients and G' is the gain factor at z=1. The filter is now in the familiar form of an IIR filter. A form of realization of a generic IIR filter is illustrated as signal-flow diagram in Fig.3.

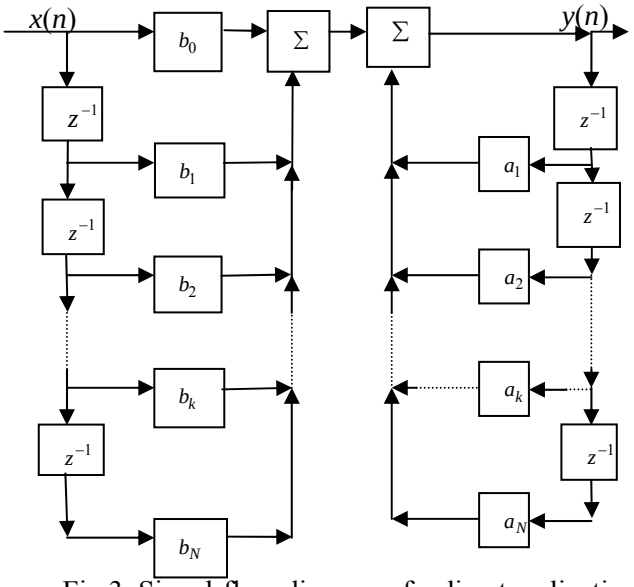

Fig.3. Signal-flow diagram of a direct realization generic infinite impulse response filter.

Following LabVIEW program based on the IIR filter for eliminating the high frequency noises was realized and the graphs concerning the input signal and the output signal processed with the IIR filter are presented in Fig.4.

2.2 Low frequency noise in the ECG

Low-frequency artifacts and base-line drift may be caused in chest-lead ECG signals by coughing or breathing with large movement of the chest. Poor contact and polarization of the electrodes may also cause low-frequency artifacts. Base line drift may sometimes be caused by variations in temperature

and bias in the instrumentation and amplifiers as well.

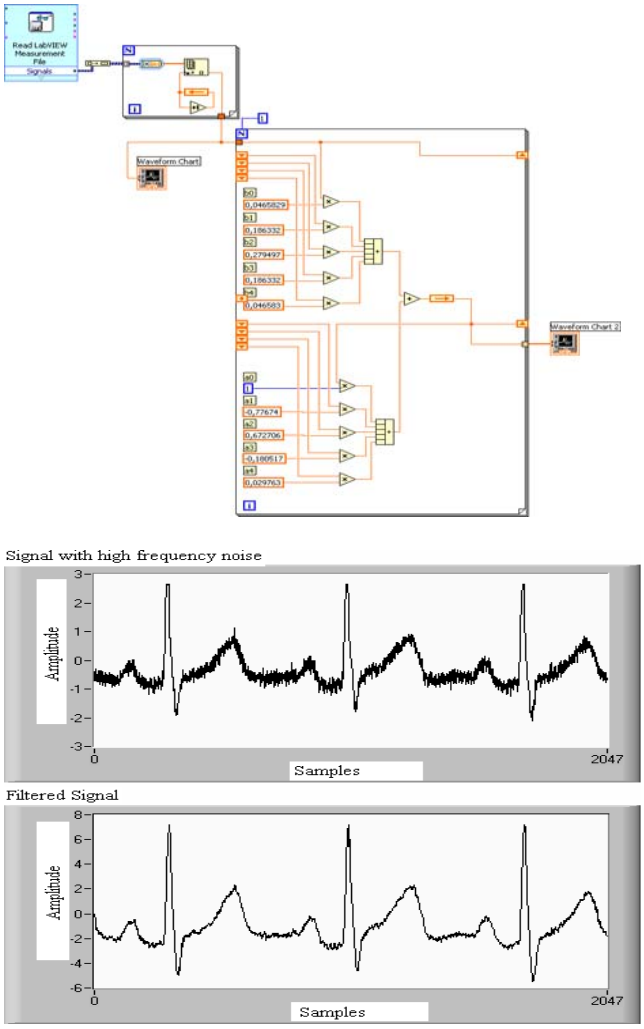

Fig.4.LabVIEW program based on IIR filter, high frequency noise signal upper graph and filtered signal lower graph (x-samples, y-amplitude).

The drawback of the first-order difference and the three-point central-difference operators [1] lies in the fact that their magnitude responses remain low for a significant range of frequencies well beyond the band related to base-line wander. We would like to maintain the levels of the components present in the signal beyond about 0.5-1Hz, that is, we would like the gain of the filter to be close to unity after about 0.5Hz. The gain of a filter at specific frequencies may be boosted by placing poles at related locations around the unit circle in the z-plane. For the sake of stability of the filter, the poles should be placed within the unit circle. Since we are interested in maintaining a high gain at very low frequencies, we could place a pole on the real axis (zero frequency), at say z=0.995 [2]. The transfer function of the modified first-order difference filter is then

$$H(z)=\frac{1}{T}\left[\frac{1-z^{-1}}{1-0.995z^{-1}}\right] \quad (6)$$

or

$$H(z)=\frac{1}{T}\left[\frac{z-1}{z-0,995}\right] \quad (7)$$

The time-domain input-output relationship is given as:

$$y(n)=\frac{1}{T}\left[x(n)-x(n-1)\right]+0,995y(n-1) \quad (8)$$

LabVIEW program and the obtained waveforms are the following, represented in Fig.5:

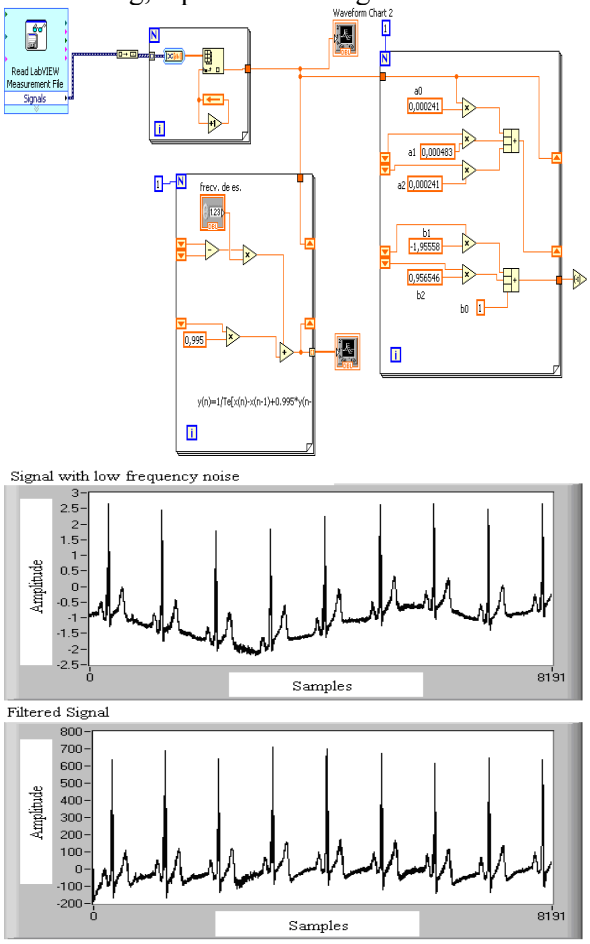

Fig.5.LabVIEW program based on the derivative operator, low frequency noise signal upper graph and filtered signal lower graph (x-samples, y-amplitude).

2.3 Power-line interference in ECG signals

The simplest method to remove periodic artifacts is to compute the Fourier transform of the signal, delete the undesired components from the spectrum, and then compute the inverse Fourier transform. The undesired components could be set to zero, or better, to the average level of the signal components over a

few frequency samples around the component that is to be removed.

Periodic interference may also be removed by notch filters [1] with zeros on the unit circle in the *z*-domain at the specific frequencies to be rejected. Applying the LabVIEW program we obtain Fig.5:

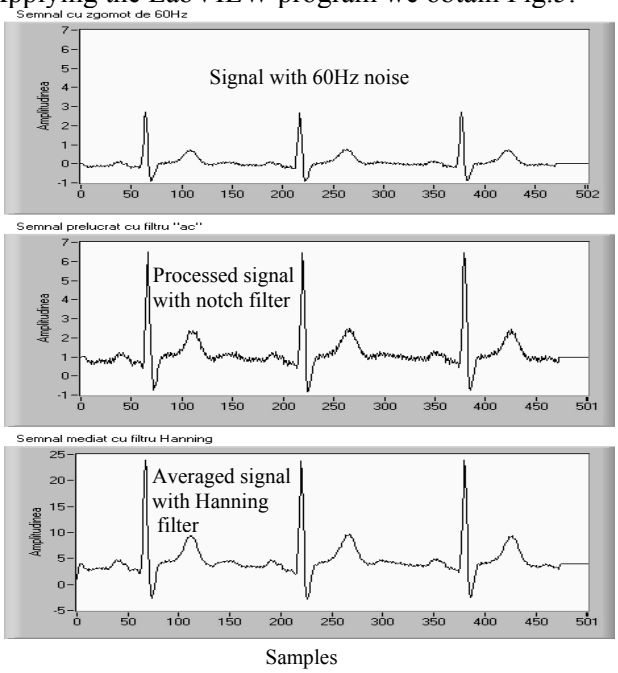

Fig. 5. Random noise elimination using notch filter and Hanning filter.

3. The Pan-Tompkins algorithm for QRS detection

Pan and Tompkins [3], [4], [5] proposed a real-time QRS detection algorithm based on analysis of the slope, amplitude and width of QRS complexes. The algorithm includes a series of filters and methods that perform lowpass, highpass, derivative, squaring, integration, adaptive thresholding and search procedures Fig.6. In this paper we implemented the Pan-Tompkins algorithm for QRS detection [1] in LabVIEW.

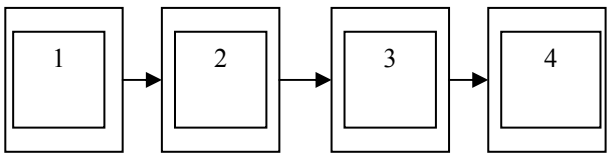

1: Band pass filter 2: Differentiator

3: Squaring operation 4: Moving-window integrator

Fig.6. Block diagram of the Pan-Tompkins Algorithm for QRS detection.

Lowpass filter: The recursive lowpass filter used in the Pan-Tompkins algorithm has integer coefficients for reducing computational complexity, with the transfer function defined as:

$$H(z)=\frac{1}{32}\cdot\frac{\left(1-z^{-6}\right)^2}{\left(1-z^{-1}\right)^2} \tag{9}$$

The output $y(n)$ is related to the input $x(n)$ as:

$$y(n)=2y(n-1)-y(n-2)+$$
$$+\frac{1}{32}\left[x(n)-2x(n-6)+x(n-12)\right]. \tag{10}$$

With the sampling rate being 200 *Hz*, the filter has a rather low cutoff frequency of f_c=11Hz, and introduces a delay of 5 samples or 24*ms*. The filter provides an attenuation greater than 35*dB* at 60*Hz*, and effectively suppresses power-line interference, if present.

Highpass filter: The highpass filter used in the algorithm is implemented as an allpass filter minus a lowpass filter. The lowpass component has the transfer function

$$H_{lp}(z)=\frac{1-z^{-32}}{1-z^{-1}} \tag{11}$$

the input-output relationship is:

$$y(n)=y(n-1)+x(n)-x(n-32). \tag{12}$$

The transfer function $H_{hp}(z)$ of the highpass filter is specified as:

$$H_{hp}(z)=z^{-16}-\frac{1}{32}H_{lp}(z). \tag{13}$$

The output $p(n)$ of the highpass filter is given by the difference equation

$$p(n)=x(n-16)-\frac{1}{32}\left[y(n-1)+x(n)-x(n-32)\right], \tag{14}$$

where $x(n)$ and $y(n)$ being related as in (12). The highpass filter has a cutoff frequency of 5*Hz* and introduces a delay of 80*ms*.

Derivative operator: The derivative operation used by Pan and Tompkins is specified as:

$$y(n)=\frac{1}{8}\left[2x(n)+x(n-1)-x(n-3)-2x(n-4)\right], \tag{15}$$

and approximates the ideal $\frac{d}{dt}$ operator up to 30 *Hz*. The derivative procedure suppresses the low-frequency components of the P and T waves, and provides a large gain to the high-frequency components arising from the high slopes of the QRS complex.

Squaring: The squaring operation makes the result positive and emphasizes large differences resulting from QRS complexes; the small differences arising from P and T waves are suppressed. The high-frequency components in the signal related to the QRS complex are further enhanced.

Integration: As observed in the previous subsection, the output of a derivative-based operation will exhibit multiple peaks within the duration of a single QRS complex. The Pan-Tompkins algorithm performs smoothing of the output of the preceding operations through a moving-window integration filter as:

$$y(n)=\frac{1}{N}\left[x(n-(N-1))+x(n-(N-2))+...+x(n)\right].(16)$$

The choice of the window width N is to be made with the following considerations: too large a value will result in the outputs due to the QRS and T waves being merged, whereas too small a value could yield several peaks for a single QRS. A window width of N=30 was found to be suitable for $f_s = 200Hz$.

Adaptive thresholding: The thresholding procedure in the Pan-Tompkins algorithm adapts to changes in the ECG signal by computing running estimates of signal and noise peaks. A peak is said to be detected whenever the final output changes direction within a specified interval. *SPKI* represents the peak level that the algorithm has learned to be that corresponding to QRS peaks and *NPKI* represents the peak level related to non-QRS events.*THRESHOLDI1* and *THRESHOLDI2* are two thresholds used to categorize peaks detected as signal or noise. Every new peak detected is categorized as a signal peak or a noise peak. If a peak exceeds *THRESHOLDI1* during the first step of analysis, it is classified as a QRS peak. Using the searchback technique the peak should be above *THRESHOLDI2* to be called a QRS. The peak levels and thresholds are updated after each peak is detected and classified as:

SPKI = 0.125*PEAKI* + 0.875*SPKI* if *PEAKI* is a signal peak;

NPKI = 0.125*PEAKI* + 0.875*NPKI* if *PEAKI* is a noise peak;

THRESHOLDI1=*NPKI* + 0.25(*SPKI* - *NPKI*);

THRESHOLDI2=0.5*THRESHOLD I1*

The updating formula for *SPKI* is changed to

SPKI = 0.25*PEAKI* + 0.75*SPKI*

If a QRS is detected in the searchback procedure [1], [3], [4] using *THRESHOLDI2.*

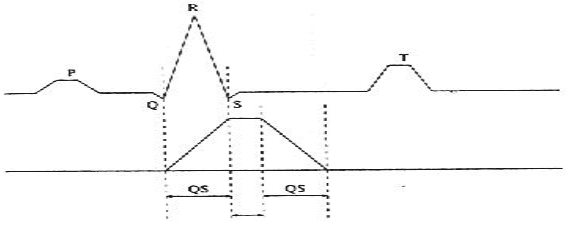

Fig.7.Upper plot-Schematic ECG signal; Lower Output of the moving-window integrator.

Fig.7 illustrates the effect of the window width on the output of the integrator and its relationship to the QRS width.

4. LabVIEW Pan-Tompkins algorithm implementation

After implementing the upper equations in LabVIEW we obtain following results Fig.8, Fig.9.

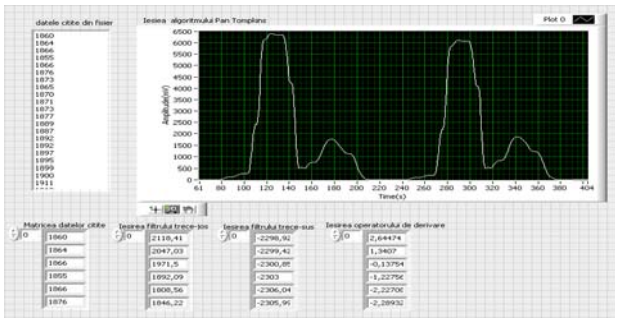

Fig.8. Pan-Tompkins algorithm front panel.

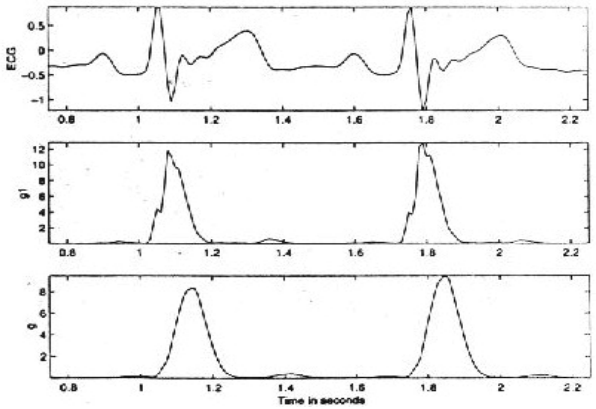

Fig.9. Results of the Pan-Tompkins algorithm.
a) two cycles of a filtered ECG;
b) output after ECG squaring;
c) the result of the final integrator.

5. QRS Detection using Adaptive Threshold

Biomedical signals are fundamental observations for analyzing the body function and for diagnosing a wide spectrum of diseases. Unfortunately, information provided by bioelectric signals is generally time-varying, nonstationary, sometimes transient, and usually corrupted by noise. One of the major areas where new insights can be expected is the cardiovascular domain. For diagnosis purpose, the noninvasive electrocardiogram is of great value in clinical practice. The ECG is composed of a set of waveforms resulting from atrial and ventricular depolarization and repolarization. The first step towards electrocardiogram analysis is the inspection of P, QRS, and T waves; each one of these

elementary components is a series of onset, offset, peak, and valley and inflection points.

Detecting QRS complexes in the ECG is one of the most important tasks that need to be performed. A real-time detection method implemented in LabVIEW is proposed, based on comparison between absolute values of summed differentiated electrocardiograms of one of more ECG leads and adaptive threshold. The threshold combines three parameters: an adaptive slew-rate value, a second value which rises when high-frequency noise occurs, and a third one intended to avoid missing of low amplitude beats [6], [9]. Two algorithms were implemented in LabVIEW: The first algorithm detects at the current beat and the second algorithm has an RR interval analysis component in addition. The algorithms are self-adjusting to the thresholds and weighting constants, regardless of resolution and sampling frequency used. They operate with any number L of ECG leads, selfsynchronize to QRS or beat slopes and adapt to beat-to-beat intervals.

The algorithm operates with a complex lead Y of several primary leads L. In cases of 12-standard leads, synthesis of the three quasi-orthogonal Frank leads is recommended first, thus determining the complex lead as a spatial vector. The complex lead is obtained as:

$$Y(i) = \frac{1}{L}\sum_{j=1}^{L} abs\left(Xj(i+1) - Xj(i-1)\right) \qquad (16)$$

where $Xj(i)$ is the amplitude value of the sample i in lead j, and $Y(i)$ is the current complex lead. This formula, except the normalizing coefficient $1/L$ and the absolute value, was initially adopted from the work of Bakardjian. Operating with unsigned, absolute values is convenient when dealing with QRSs and extrasystoles having different, for example positive in one lead and negative in the other lead deflections.

Adaptive steep-slope threshold – S

Initially $S = 0.7*max(Y)$ is set for the first 5 s of the signal, where at least two QRS complexes should occur. A buffer with 5 steep-slope threshold values is preset:

$$SS = [S1\,S2\,S3\,S4\,S5], \qquad (17)$$

where $S1 \div S5$ are equal to S. QRS or beat complex is detected if $Yi \geq SIB$, where the differentiated and summed signals from L leads are compared to the absolute value of a threshold that is $SIB=S+I+B$, a combination of three independent adaptive thresholds: *S – Steep slope threshold, I – Integrating threshold for high frequency components, B – Beat expectation threshold.*

No detection is allowed 300 ms after the current one. In the interval QRS ÷ QRS+300*ms* a new value of S_5 is calculated:

$$newS5 = 0.7*max(Yi). \qquad (18)$$

The estimated *newS5* value can become quite high, if steep slope premature ventricular contraction or artifact appeared, and for that reason it is limited to $newS5 = 1.2*S5$ if $new\ S5 > 1.6*S5$. The *SS* buffer is refreshed excluding the oldest component, and including $S5 = newS5$. *M* is calculated as an average value of *SS*. *S* is decreased in an interval 300 to 1300 ms following the last QRS detection at a low slope, reaching 70 % of its refreshed value at 1300 ms. After 1300 ms *S* remains unchanged. The thresholds definitions are presented in more detail with the help of several examples. Two ECG leads are shown in Fig.10. Detected QRSs are marked with 'red O' on Lead 1. The summary lead and the steep-slope threshold are represented in Fig.11. The algorithm was implemented using LabVIEW.

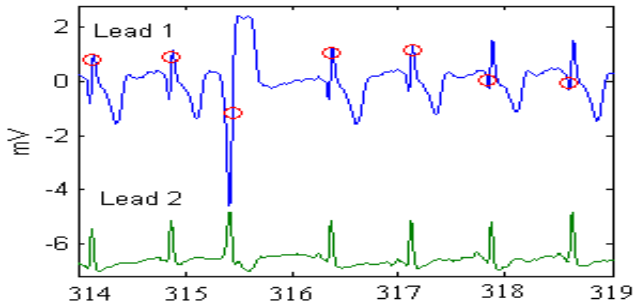

Fig.10. Adaptive steep-slope threshold with two ECG leads.

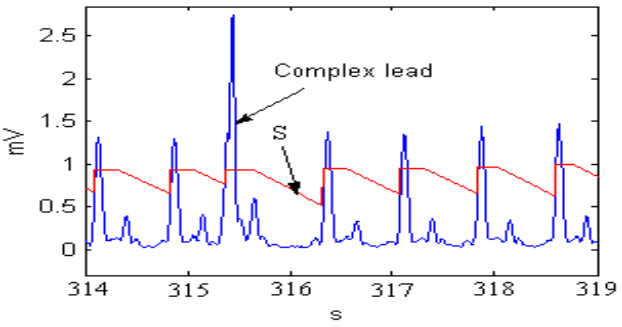

Fig.11. Adaptive steep-slope threshold with summary lead and steep-slope threshold.

Adaptive integrating threshold – I

The integrating threshold *I* is intended to raise the combined threshold if electromyogram noise is accompanying the ECG, thus protecting the algorithm *against erroneous beat detection*. Initially *I* is the mean value of the pseudo-spatial velocity *Y* for 350 ms. With every signal sample, *I* is updated adding the maximum of *I* in the latest 50 ms of the 350 ms interval and subtracting *maxY* in the earliest

50 ms of the interval. It is possible to represent this in equation (19)

I = I + (max(Yin latest 50 ms in the 350 ms interval) - max(Yin earliest 50 ms in the 350 ms interval))/150.

The way *I* is updated means that not every sample in the interval is integrated, but just the envelope of the pseudospatial velocity *Y*. The weight coefficient 1/150 is empirically derived. Two ECG leads are shown in Fig.12. The pseudo-spatial velocity *Y* and the integrated threshold are presented in Fig.13. The correct detection is due to the rise of *I* with about 0.2 mV. The beat complex is included in the integration process, thus making almost impossible a close detection to the previous complex. It is possible to observe the high rise of *I* after any of the complexes. The algorithm was implemented using LabVIEW.

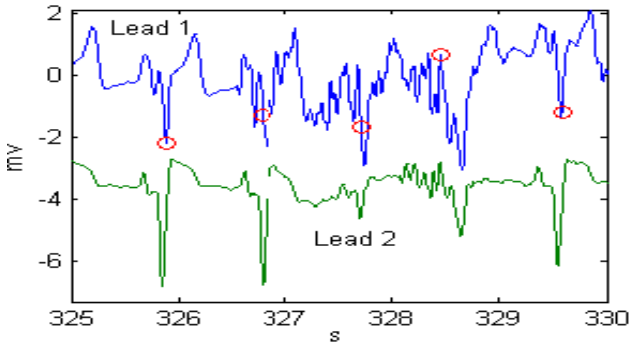

Fig.12. Adaptive integrating threshold with two ECG leads.

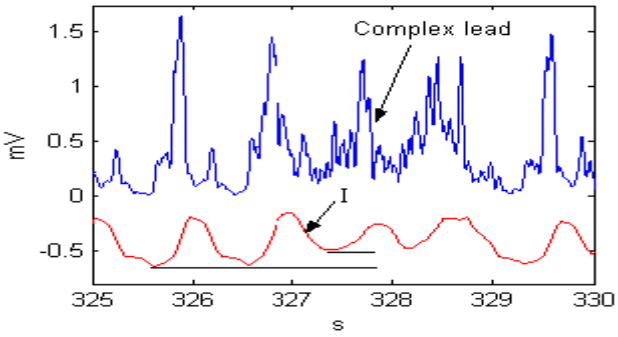

Fig.13. Adaptive integrating threshold with pseudo-spatial velocity and threshold representation.

6. Beat detection algorithms

The QRS complexes and ventricular beats in an electrocardiogram represent the depolarization phenomenon of the ventricles and yield useful information about their behavior. Beat detection is a procedure preceding any kind of ECG processing and analysis.

A crucial part of any ECG processing algorithm is beat detection. Beat detection algorithms typically incorporate a preprocessing filter which decomposes the ECG into a signal which maximizes the signal-to-noise ratio of the QRS complex. A nonlinear processing stage and moving window integrator are used to compute a signal that emphasizes the energy of the QRS complex. Beat detection logic incorporates a history of signal peaks which are used to establish signal and noise levels, respectively. A threshold is then used to decide if an incoming peak is due to the QRS complex or noise. If a period of time corresponding to the average heartbeat interval elapses without a beat detection a *back-search* strategy is used to check the ECG again for the presence of a beat. The described algorithm operates at the same rate as the input ECG. The used filters are designed to optimize the SNR of the QRS complex. The information from other frequency components of the ECG is filtered out and cannot be incorporated into the beat detection logic. Thus, the preprocessing filters are not useful to other ECG processing tasks. Preprocessing means a moving averaging filter for power-line interference suppression, that averages samples in one period of the power line interference frequency with a first zero at this frequency [7], [10].

Adaptive beat expectation threshold – B

The beat expectation threshold *B* is intended to deal with heartbeats of normal amplitude followed by a beat with very small amplitude and respectively with very small slew rate. This can be observed for example in cases of electrode artifacts. Conversely to the integrating threshold protecting against erroneous QRS detection, *B* is protecting against *QRS misdetection*.

The effect of the threshold values and the type of features on the beat detection accuracy was studied. The beat detection accuracy of a one-channel detection block was computed using various threshold values, and both the sum-of-square and sum of- absolute features discussed above. From this analysis the threshold values can be strategically chosen to provide beat detection blocks with complementary detection rates. A buffer with the 5 last *BB* intervals is updated at any new QRS detection. *Bm* is the mean value of the buffer. *B* = 0*V* in the interval from the last detected QRS to 2/3 of the expected *Bm*. In the interval QRS + *Bm* * 2/3 to QRS + *Bm*, *B* decreases 1.4 times slower then the decrease of the previously discussed steep slope threshold (*S* in the 300–1300 ms interval). After we obtain QRS + *Bm* the decrease of *B* is stopped. The time-course of the beat expectation threshold *B* is shown in Fig. 14.

The decrease of *B* with about 0.2 mV at the fourth QRS allows its detection, despite the lack of complex in Lead 2, which leads to a two-fold decrease of the summary lead amplitude *Y* as in Fig.15. The algorithm was implemented using LabVIEW.

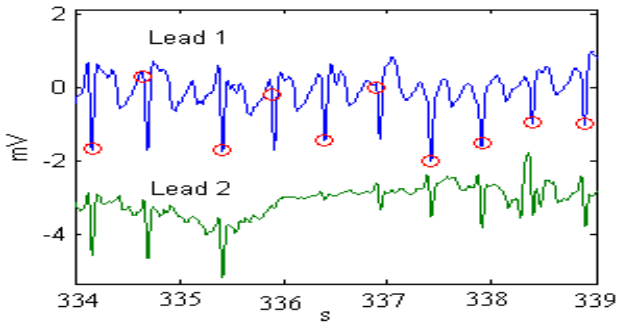

Fig.14. Adaptive beat expectation threshold with two leads.

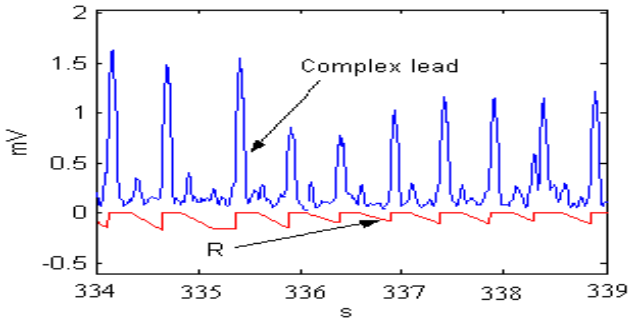

Fig.15. Adaptive beat expectation threshold with complex lead and threshold representation.

Fig. 16 gives an overview of the sequential levels in the beat detection algorithm. The goal of the detection algorithm is to maximize the number of true positives, while keeping the number of false negatives and false positives to a minimum. Since it is not possible to arrive at this goal using one simple detector, multiple detectors with complementary false negatives and false positives performances are simultaneously operated and the results of each fused together to arrive at an overall decision.

The advantage of this strategy is that multiple features which are indicative of the QRS complex can be used to detect beats. A nonlinear processing stage and *moving window integrator (MWI)* are used to compute a signal that emphasizes the energy of the QRS complex. Beat detection logic incorporates a history of signal peaks and noise peaks which are used to establish signal and noise levels, respectively. A threshold is then used to decide if an incoming peak is due to the QRS complex or noise. The event detector flags an event when a peak occurs in the output of a *MWI* operating on an existing feature. The beat detection process occurs at a subband rate instead of the input ECG rate. In a one-channel beat detection algorithm, the threshold value determines the classification of an incoming feature as a signal peak or noise peak. A low threshold will result in noise peaks being classified as a beat, and the feature value updated in the signal history. This will result in an inaccurate estimated signal level. However the noise history is updated accurately since the low threshold does not allow signal peaks to be incorrectly detected as noise. Similarly a high threshold will incorrectly result in some signal peaks being classified as noise and updated in the noise history. This will incorrectly raise the noise level and affect future beat detections. However in this way the signal history is updated accurately since beat detections using a high threshold are most likely correct.

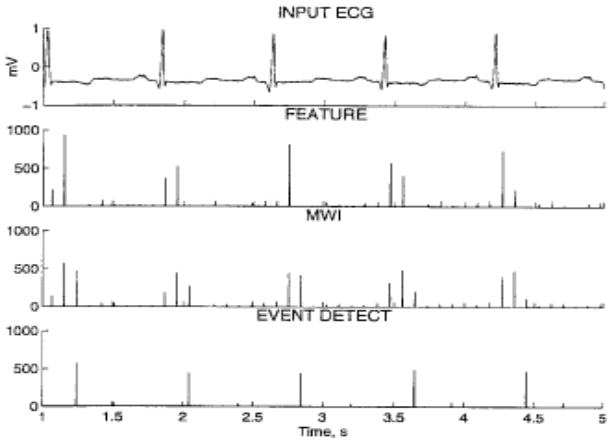

Fig. 16. ECG, ECG computed feature, MWI output, event detector output.

The effect of the threshold values and the type of features on the beat detection accuracy was studied. The beat detection accuracy of a one-channel detection block was computed using various threshold values, and both the sum-of-square and sum of-absolute features discussed above. From this analysis the threshold values can be strategically chosen to provide beat detection blocks with complementary detection rates that means one with minimal false positives, and the other with minimal false negatives. Beat detection performance for a one-channel beat detection block was studied using different databases for various features and threshold values. Based on these preliminary studies we noted that, in general, the sum-of-square features generate less false positives and more false negatives for the same threshold value than the sum-of-absolute features. This fact may be useful in a beat detection algorithm which uses multiple, complementary features such as these.

7. Cardiac Beat Recognition based on Wavelet Transform

Wavelet transforms [2], [8] have been applied to electrocardiogram signals for enhancing late potentials, reducing noise, and QRS detection, normal and abnormal beat recognition. In this paper the continuous wavelet transform *CWT* based on a complex analyzing function is applied to characterize local symmetry of signals and it is used for ECG arrhythmia analysis. The continuous wavelet transform *CWT* of a signal *f* belonging to $\boldsymbol{L^2(\mathcal{R})}$ is defined by:

$$(W_\Psi f)(a,b) = \frac{1}{\sqrt{a}} \int_{-\infty}^{+\infty} f(t)\overline{\Psi\left(\frac{t-b}{a}\right)}dt \qquad (19)$$

where Ψ is a complex valued function with zero mean and satisfying $C_\Psi < \infty$

$$C_\Psi = 2\pi \int_{-\infty}^{+\infty} |\omega|^{-1} \left|\hat{\Psi}(\omega)\right|^2 d\omega < \infty \qquad (20)$$

in effect, if $\Psi \in \boldsymbol{L_1 \cap L_2}$. The analyzed signal $f(t)$ is real and supposed to be two times continuously differentiable. Basically, hidden Markov models are doubly stochastic processes that can characterize any discrete sequence of feature vectors $\{\boldsymbol{o_t}\}_{1 \le t \le T}$, derived from an input signal *f(t)* and considered as realizations of so-called *observable process*. The modeling technique described here considers the observed ECG signal *f(t)* as being equivalent to a sequence of events associated with state changes. A *CWT* technique is proposed to classify normal sinus rhythm (NSR) and various cardiac arrhythmias including atrial premature contraction (APC), premature ventricular contraction (PVC), superventricular tachycardia (SVT), ventricular tachycardia (VT) and ventricular fibrillation (VF). Analyzing the local maxima lines using the *CWT* technique it is possible to diagnose with accuracy the above disfunctionalities.

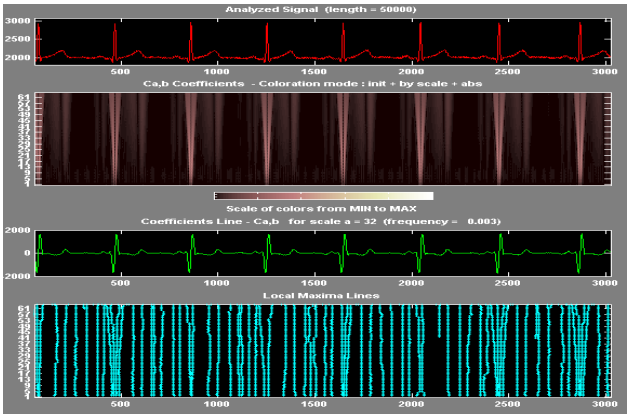

Fig.17. *CWT* analysis of an electrocardiogram.

8. Conclusion

The results obtained using LabVIEW for the implementation of the Pan-Tompkins algorithm is very fast and useful, because the ECG can be easily read and saved in a file and the filtering, squaring, integrating, applying the moving window can be accurately done. The peak detection is very important in diagnostic decision.

The proposed algorithms for real-time and pseudo-real time implementation are adaptive, independent of thresholds and constants values. They are self-synchronized to the QRS steep slope and the heart rhythm, regardless of the resolution and sampling frequency used.

The beat detection accuracy of the algorithm is comparable to other algorithms reported in the literature. The large variety of QRS detection algorithms, and the continuous efforts for their enhancement, proves that universally acceptable solution has not been found yet. Difficulties arise mainly from the huge diversity of the QRS complex waveforms and the noise and artifacts accompanying the ECG signals.

References:

[1]Rangayyan R.M., *Biomedical Signal Analysis*, Wiley-Intersciene, John Wiley & SONS, INC., 2002.

[2]Aldroubi A., Unser M., *Wavelets in Medicine and Biology*,CRC Press, Florida, 1996.

[3]Boashash B., *Time-Frequency Signal Analysis.*Wiley, New York, NY,1992.

[4]Pan J. and Tompkins WJ., *A real-time QRS detection algorithm*, IEEE Transactions on Biomedical Engineering, pp:230-236, 1985.

[5]Tompkins WJ., *Biomedical Digital Signal Processing*, Prentice-Hall, Upper Saddle River, NJ, 1995.

[6] Christov I.I., *Real time electrocardiogram QRS detection*, BioMedical Engineering OnLine.

[7] Bakardjian H., *Ventricular beat classifier using fractal number clustering***,** Med Biol Eng Comput 1992, pp**:**495-502.

[8] Li C., Zheng C., Tai C., *Detection of ECG characteristic points using wavelet transforms***,** IEEE Trans on Biomed Eng 1995, pp**:**21-28.

[9] Moreas J.C., Seixas M.O., Vilani F.N., Costa E.V., *A QRS complex detection algorithm using electrocardiogram leads***,** Comp in Card 2002, pp**:**205-208.

[10] Afonso V. X., Tompkins W.J., Nguyen T.Q., Luo S., *ECG Beat Detection Using Filter Banks*, IEEE Transactions on Biomedical Engineering,Vol.46, No.2, February 1999.